



# Energy Dissipation-Based Method for Fatigue Life Prediction of Rock Salt

Mingming He<sup>1</sup> · Bingqian Huang<sup>2</sup> · Caihui Zhu<sup>1</sup> · Yunsheng Chen<sup>1</sup> · Ning Li<sup>1,3</sup>

Received: 21 June 2017 / Accepted: 4 January 2018 / Published online: 20 January 2018  
© Springer-Verlag GmbH Austria, part of Springer Nature 2018

## Abstract

The fatigue test for rock salt is conducted under different stress amplitudes, loading frequencies, confining pressures and loading rates, from which the evaluation rule of the dissipated energy is revealed and analysed. The evolution of energy dissipation under fatigue loading is divided into three stages: the initial stage, the second stage and the acceleration stage. In the second stage, the energy dissipation per cycle remains stable and shows an exponential relation with the stress amplitude; the failure dissipated energy only depends on the mechanical behaviour of the rock salt and confining pressure, but it is immune to the loading conditions. The energy dissipation of fatigued rock salt is discussed, and a novel model for fatigue life prediction is proposed on the basis of energy dissipation. A simple model for evolution of the accumulative dissipated energy is established. Its prediction results are compared with the test results, and the proposed model is validated.

**Keywords** Rock salt · Fatigue life prediction · Energy dissipation

## List of symbols

$E_o$	Total dissipated energy
$E_d$	Energy dissipated by storage wall damage
$E_h$	Heat energy mainly dissipated by chemistry, conduction and radiation
$W_d^i$	Dissipated energy of cycle $i$
$\varepsilon_i$	Strain amplitude of cycle $i$
$A$	Stress amplitude
$W_d^i$	Dissipated energy of cycle $i$
$W_d^{i+1}$	Dissipated energy of cycle $i + 1$
DER	Dissipated energy ratio
$w_d$	Stable energy dissipation per cycle
$\mu$	Loading rate
$\nu$	Loading frequency
$a, b$ and $c$	Curve-fitting parameters for the rock salt $w_d$ curve
$N$	Cycle number

$N_f$	Fatigue life
$W_f$	Accumulative dissipated energy when the specimen fractures
$\xi$	Material constant $\xi = \frac{w_d N_f}{W_f}$
$W_f^1$	Accumulative dissipated energy at the initial stage of fatigue loading
$W_f^2$	Accumulative dissipated energy at the second stage of fatigue loading
$W_f^3$	Accumulative dissipated energy at the acceleration stage of fatigue loading

## 1 Introduction

Rock salt is a kind of natural material in energy engineering. With the mechanical behaviours of low strength and large deformation, as well as the physical characteristics of tightness and stability, rock salt has been used as a favoured medium for waste disposal and oil and gas storage since the last century, when it began to be widely investigated (Liang et al. 2011). During its lifetime, a storage cavern of rock salt is influenced mainly by the periodic injection and extraction of frequently encountered gas (Liang et al. 2012). The periodic injection and extraction actually lead to exchanging energy with the environment throughout the loading process on the storage walls. For the long-term stability analysis

✉ Mingming He  
807658619@qq.com

<sup>1</sup> Institute of Geotechnical Engineering, Xi'an University of Technology, Xi'an 710048, China

<sup>2</sup> College of Information Engineering and Automation, Kunming University of Science and Technology, Kunming 650500, China

<sup>3</sup> School of Civil Engineering, Lanzhou Jiaotong University, Lanzhou 730070, China

of a permanent repository, a fatigue theory is required that allows, on the basis of laboratory results, one to predict the fatigue life of the rock salt storage walls with high reliability. Therefore, it is of vital importance to investigate the fatigue life in practical applications of rock salt, which could effectively assist in designing and estimating the fatigue life of gas storage facilities more rationally.

Up to now, many fatigue life prediction methods for rock salt have been developed. Two approaches are usually used to investigate the fatigue failure mechanism of rock salt: the damage theory and the S–N method (Guo et al. 2012; Song et al. 2013; Ma et al. 2017).

The S–N method makes use of the fatigue life data from lots of fatigue tests and establishes a representative empirical model for the S–N curve through regression analysis (Song et al. 2013). The S–N method for lifetime prediction of fatigued material is reliable and simple; hence, it has currently become the main method for fatigue life prediction. However, the S–N method suffers from the discreteness of rock salt properties and the failure behaviour being neglected. The damage theory makes use of a number of variables to describe the damage of materials (Guo et al. 2012; Xiao et al. 2010; Ma et al. 2017) and then establishes the corresponding damage evolution model and constitutive relation (Xiao et al. 2009). The energy method analyses the development of dissipated energy in the process of fatigued materials, from which it then reveals the damage evolution law and proposes the prediction model for fatigue life (Lei et al. 2008; Wang et al. 2016; Xiao and Gu 1998).

The purpose of this work is to investigate the fatigue life of rock salt with the energy method and to explore the effect of amplitude, loading frequency and loading rate on the fatigue life. Through lots of fatigue tests of rock salt and analysing the energy dissipation in the fatigue loading process, the evolution laws of energy dissipation are put forward, and a novel prediction method for the fatigue life of rock salt is proposed.

## 2 Energy Parameters for the Fatigue Process

### 2.1 Energy Analysis of the Fatigue Process

Rock salt in the storage wall is always exchanging energy with the environment due to the injection and withdrawal of storage product. When injected periodically and extracted frequently, the waste disposal and oil and gas in a storage cavern of rock salt do work on the storage walls. Part of the mechanical energy dissipates as heat, and the other energy is stored in the walls as internal energy. Regarding the storage and the storage walls of rock salt as a dissipative system, the amount of dissipated energy is equal to the decrement of work capacity, from the dissipation systems theory. The elastic deformation

is recoverable; hence, all the energy except the elastic deformation energy is the dissipated energy of the system, such as the irrecoverable plastic deformation energy, the heat energy and the chemical energy. The total dissipated energy can be divided into two parts, including the heat energy mainly dissipated by chemistry, conduction and radiation (Qian et al. 2010; Xie et al. 2011) and the dissipated energy due to storage wall damage. During the cycling of periodic injection and frequent extraction, if the loading rate remains constant, the heat energy is regarded as invariant at the same temperature, and the former is small in comparison with the latter (Xie et al. 2004, 2005, 2011). The total dissipated energy can be expressed as

$$E_o = E_d + E_h \quad (1)$$

where  $E_o$  is the total dissipated energy,  $E_d$  is the energy dissipated by storage wall damage, and  $E_h$  is the heat energy mainly dissipated by chemistry, conduction and radiation (Qian et al. 2010; Xie et al. 2011).

The usual energy dissipated by damage includes the plastic strain energy absorption and the energy dissipated by crack propagation and defect formation. The corresponding physical quantities, hence, have been selected as the fatigue damage variables to describe the degree of material damage (Payten et al. 2010). As is shown in experiments (Datoma and Giancane 2013), the heat energy dissipation in the fatigue loading process is regarded as invariant at the same test temperature generally, and the trend of energy dissipated by the damage is almost the same as that of the total energy dissipation. Hence, the total dissipated energy can be represented by the energy dissipated by damage, both of which are regarded as the dissipated energy in this paper.

### 2.2 Dissipated Energy

According to the definition of dissipated energy, the dissipated energy per cycle is equal to the work decrement of the dissipative system in fatigue loading and is generally regarded as the area of the hysteresis curve:

$$W_d^i = \oint \sigma_i d\varepsilon_i \quad (2)$$

where  $W_d^i$  is the dissipated energy of cycle  $i$ ,  $\varepsilon_i$  is the strain amplitude of cycle  $i$ , and  $\sigma_i$  is the stress amplitude. Due to the increase in the dissipated energy in the process of fatigue loading, the accumulated plastic dissipation energy equals the summation of energy dissipation per cycle from the beginning of fatigue loading to the current cyclic number  $N$ :

$$W_d = \sum_{i=1}^N W_d^i \quad (3)$$

The dissipated energy is dependent on the loading cycle history; hence, the DER (dissipated energy ratio) is proposed

on the basis of the change in dissipated energy, which means the fluctuation of energy dissipation between two neighbouring cycles, and can be calculated as (Shen et al. 2006; Ghuzlan and Carpenter 2006):

$$\text{DER} = (W_d^{i+1} - W_d^i) / W_d^i \quad (4)$$

where  $W_d^i$  is the dissipated energy of cycle  $i$ , and  $W_d^{i+1}$  is the dissipated energy of cycle  $i + 1$ .

### 3 Fatigue Test

#### 3.1 Test Equipment

The compression–compression fatigue tests were conducted on the WDT-1500 Rock Test System with a load capacity of 1500 kN, confining pressure capacity of 80 MPa and frequency capacity of 10 Hz (see Fig. 1). The WDT-1500 controller consists of a hardware component and software applications. It has four main parts: a digital servo controller, an axial dynamic loading system, a self-balanced pressure chamber and a data acquisition system. The computer is used to control the host to run the experiment.

#### 3.2 Test Specimen

The rock salt samples in this experiment were obtained from a salt mine in the Shanbei region, Shanxi Province of China (see Fig. 2). The rock salt has very high purity (NaCl and Na<sub>2</sub>SO<sub>4</sub>), with a spot of K<sub>2</sub>SO<sub>3</sub>. To ensure the trustworthiness of the experimental results as much as possible, we selected non-joint samples with almost the same purity. The samples were cut into standard cylinders 50 mm in diameter and 100 mm in length according to the ISRM testing procedure and guidelines.

#### 3.3 Test Method

To determine the stress level applied in the fatigue test, the static compressive strength of the sample was 65.3 MPa by being tested at a loading rate of 0.1 kN/s. In the compression–compression fatigue test, the upper levels in this experiment, defined as the ratio of upper stress to static compressive strength, were set to 0.95. To investigate the effect of the loading frequency, loading rate, confining pressure and stress amplitude on the fatigue behaviour of rock salt, the compression–compression fatigue tests were subjected to four cyclic loading schemes (Table 1): different loading frequencies (0.5, 1, 2 and 4 Hz), different loading rates (0.5, 1, 2, 4 and 8 kN/s), different stress amplitudes (7.64, 15.2, 30.57, 45.86 and 61.15 MPa) and different confining pressures (1, 5 and 8 MPa). At the beginning of the test, the rock salt sample was loaded to the set upper level of 0.95, which was similar to the static loading. Then, the fatigue test was conducted with a harmonious sinusoidal cyclic pressure load. Under fatigue loading, the corresponding strain curve is shown in Fig. 3, in which the upper strain stands for the maximum strain at the current cyclic number  $N$ . The lower strain stands for the minimum strain at the current cyclic number  $N$ . The fatigue compression strain is compared to static creep tests performed under similar conditions, which are characterized by the three stages of deformation (Roberts et al. 2015).

The test machine is set to acquire a complete cycle of data on the stress and strain for each cycle, collecting all data points from the beginning of fatigue loading to fatigue failure. Corresponding hysteresis curves can be obtained. According to Eq. (2), the area is calculated by the numerical integration of the hysteresis curve, which is the energy dissipation per cycle.



Fig. 1 Specimens before and after the cyclic loading test

**Fig. 2** WDT-1500 Rock Testing System



**Table 1** Summary of the samples tested and the test results of the accumulative dissipated energy  $W_f$  when the specimen fractures, accumulative dissipated energy  $W_f^1$  at the initial stage of fatigue loading, accumulative dissipated energy  $W_f^2$  at the second stage and accumulative dissipated energy  $W_f^3$  at the acceleration stage

No.	A (MPa)	$\nu$ (Hz)	$\mu$ (kN/s)	$\sigma_3$ (MPa)	$N_f$	$W_f$ (kJ m <sup>-3</sup> )	$W_f^1$ (kJ m <sup>-3</sup> )	$W_f^2$ (kJ m <sup>-3</sup> )	$W_f^3$ (kJ m <sup>-3</sup> )
S1	7.64	1	1	0	223	235	15.3	195.2	24.5
S2	15.29	1	1	0	132	231	17.5	187.7	25.8
S3	30.57	1	1	0	57	234	16.4	193.2	24.4
S4	45.86	1	1	0	42	229	15.8	186.4	26.8
S5	61.15	1	1	0	17	238	17.2	195.7	25.1
S6	15.29	1	0.5	0	277	234	16.7	192.9	24.4
S7	15.29	1	1	0	138	226	18.4	186.3	21.3
S8	15.29	1	2	0	68	231	15.6	191.3	24.1
S9	15.29	1	4	0	39	234	17.3	192.3	24.4
S10	15.29	0.5	1	0	299	231	16.2	190.4	24.4
S11	15.29	1	1	0	132	228	14.9	186.5	26.6
S12	15.29	2	1	0	55	238	16.4	196.7	24.9
S13	15.29	4	1	0	38	240	17.3	196.2	26.5
S14	15.29	1	8	0	18	237	15.7	195.3	26.0
S15	15.29	1	1	1	158	256	20.3	207.5	28.2
S16	15.29	1	1	5	285	395	30.2	321.5	43.3
S17	15.29	1	1	8	403	512	38.6	412.3	61.1

## 4 The Evolution of the Energy Dissipation Under Fatigue Loading

### 4.1 The Evolution Rule of the Energy Dissipation Per Cycle

Three stages in energy dissipation development are shown in Fig. 4 and are characterized as follows: in the first stage, the dissipated energy per cycle descends slowly during the first few cycles; after a number of cycles, the dissipated energy tends to be stable, and its value is regarded as invariant; and

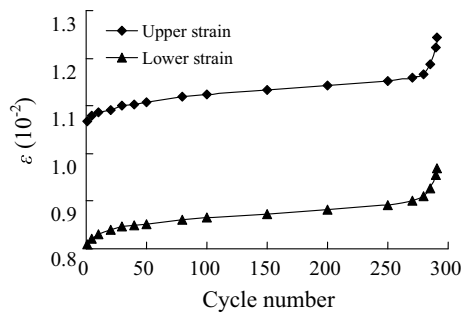


**Fig. 3** The upper strain and lower strain-cycle number curve under fatigue loading

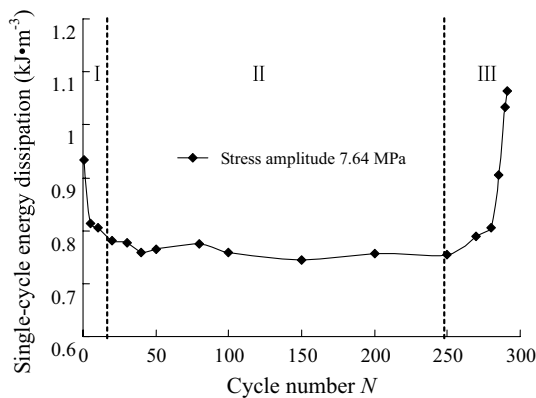


**Fig. 4** Evolution of energy dissipated per cycle for No.S1 specimen at the stress level of 0.95

in the final stage, the dissipated energy per cycle increases rapidly until the specimen of rock salt fractures.

The rock salt consists of crystal grains of various geometry and texture (Hakan 2009). The opened and closed boundaries of these grains are called the original in situ crack condition. The original cracks and the secondary cracks originated by the first static loading cannot be neglected during the process of fatigue loading. At the initial stage of fatigue loading, the dissipated energy per cycle by damage decreases rapidly due to the gradual compression of the specimen resulting in the decrease of porosity. The heat energy dissipation caused by the sliding friction and dislocation processes (Hakan 2009) among the boundaries of these crystal grains is in a downward trend due to the closure of some primary pores and cracks and secondary cracks with increasing compaction, so the total energy dissipation shows a downward trend. When the specimen is compacted fully, the total energy dissipation shows no obvious downward trend as shown in Fig. 4.

In the second stage, micro-defects and micro-cracks start to appear ceaselessly in the interior of the specimen,

but are not enough to form macroscopic cracks. Thus, the specimen is under a metastable state, and the energy dissipation remains stable for each cycle, implying that the energy dissipation per cycle is immune to the current damage of the rock salt.

Micro-fracturing has been found to be the principle mechanism of fatigue failure in fatigue loading (Erarslan 2016). In the final stage (acceleration stage), it appears that the microstructure of the rock, such as the initiating and propagating fatigue cracks, has an effect on the fatigue characteristics. Hence, the energy dissipation per cycle increases rapidly, until reaching a critical value that directly leads to the fatigue failure of the tested specimen.

The following is evident: the energy dissipation decreases rapidly during the initial stage; after some cycles, the rate of energy dissipation tends to be stable; and near failure, the energy dissipation increases rapidly again to eventual fatigue failure. Notably, the total dissipated energy of the second stage under different applied stress amplitudes, loading frequencies and loading rates is distributed evenly between 186.3 and 196.2  $\text{kJ m}^{-3}$ , and then the total dissipated energy of the initial stage and acceleration stage is distributed evenly between 39.7 and 43.3  $\text{kJ m}^{-3}$  as shown in Table 1. This suggests that the total dissipated energy of the initial stage and acceleration stage is nearly constant. In addition, it is found that during fatigue loading, the total dissipated energy of the second stage is much more than that of the initial and acceleration stages, representing the majority of the energy dissipation when the fatigue test of rock salt was conducted. This may be due to the fact that at the initial stage of cyclic loading, the hysteretic circle is sparse, and then it becomes more and more close; and finally, the hysteretic circle changes back to sparse. It presents a stage of sparseness–closeness–sparseness (Guo et al. 2012; Kittitep and Decho 2010).

The stable energy dissipation per cycle also changes with the loading conditions. The development of the stable energy dissipation per cycle is dependent on the applied stress amplitude, loading frequency, loading rate and confining pressure. The energy dissipation per cycle at a constant stress level of 0.95 under different applied loading conditions can be obtained as shown in Fig. 5, and then the exponential function is used to fit the relation between the applied stress amplitude, loading frequency, loading rate and confining pressure, as shown in Fig. 6; the fitting function is

$$w_d = c(\mu v)^a \exp [b(A - \sigma_3)] \tag{5}$$

where  $w_d$  is the stable energy dissipation per cycle,  $\mu$  is the loading rate in  $\text{kN/s}$ ,  $v$  is loading frequency in  $\text{Hz}$ ,  $A$  is the stress amplitude in  $\text{MPa}$ , and  $a$ ,  $b$  and  $c$  are fitting coefficients  $a = 1.0012$ ,  $b = 0.047$ , and  $c = 0.576$ , respectively.

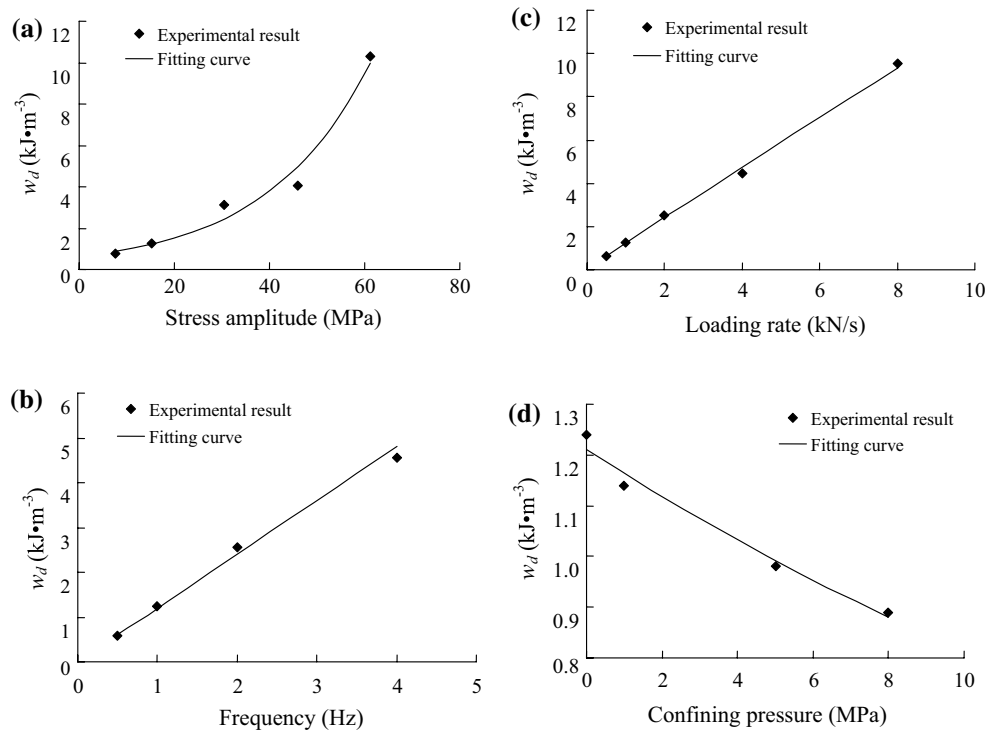


Fig. 5 The relationship between the stable energy dissipation per cycle  $w_d$  and the applied loading

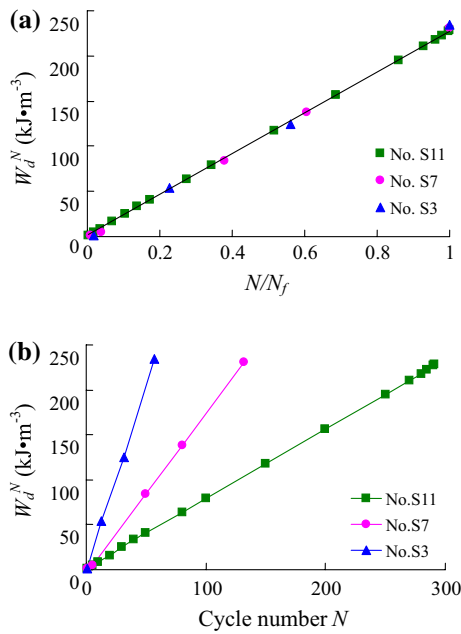


Fig. 6 The relation between the accumulative dissipated energy  $W_d^N$  and cycle number and cycle ratio  $N/N_f$

### 4.2 The Evolution of Accumulative Dissipated Energy

The curve of accumulative dissipated energy  $W_d^N$  at the current cyclic number  $N$  under different loading conditions is obtained by Eq. (3) as shown in Fig. 6a. It is obvious that the accumulative dissipated energy  $W_d^N$  increases linearly with cycle number  $N$ , and the larger the applied stress amplitude, loading frequency and loading rate are, the faster  $W_d^N$  increases. It is worth noting that accumulative dissipated energy  $W_d^N$  also increases linearly as the cycle ratio  $N/N_f$  ( $N_f$  is fatigue life), and unlike the relationship between the accumulative dissipated energy and cycle number, there is no effect of the applied stress amplitude, loading frequency and loading rate on the relationship between the accumulative dissipated energy and cycle ratio, even at the entire process of fatigue loading as shown in Fig. 6b. Therefore, the accumulative energy dissipation could be used as the variable to describe the rock damage (Ghuzlan and Carpenter 2006; Erarslan 2016). Hence, the accumulative dissipated energy  $W_d^N$  at the current cyclic number  $N$  can be expressed as

$$W_d^N = W_f \frac{N}{N_f} \tag{6}$$

where  $N$  is the cycle number,  $N_f$  is fatigue life, and  $W_f$  is the accumulative dissipated energy when the specimen fractures

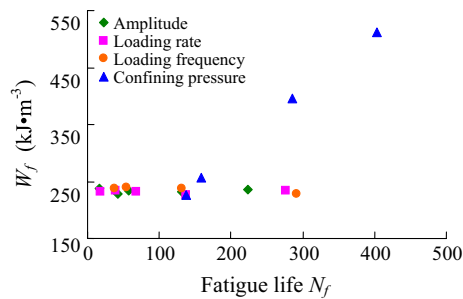


**Fig. 7** The relation between the failure dissipated energy  $W_f$  and fatigue life

defined as the failure dissipated energy. The failure dissipated energy  $W_f$  refers to the accumulative dissipated energy when fatigue fracture occurs in the specimen of rock salt. In this paper, the fatigue tests are carried out on seventeen specimens of rock salt with identical strength, the evolution curve of the energy dissipation under different loading conditions is obtained, and the corresponding failure energy dissipation is summarized, as shown in Fig. 7. The failure energy dissipation  $W_f$  under different applied stress amplitude, loading frequency and loading rate is distributed evenly between 226 and 241  $\text{kJ m}^{-3}$ , and there is no obvious relation between  $W_f$  and the loading conditions. It is concluded that the failure accumulative energy dissipation  $W_f$  is constant at the same confining pressure and invariable and independent of the applied stress amplitude, loading frequency and loading rate. Thus, the failure dissipated energy  $W_f$  can be regarded as a failure criterion for rock salt fatigued under uniaxial loading.

Table 1 shows the fatigue and dissipated energy properties of the rock salt samples under confining pressure. The rock salt specimen tests showed that the fatigue life increases with higher confining pressure: for confining pressures of 0, 1, 5 and 8 MPa, the fatigue life of the rock salts was 138, 158, 285 and 403, respectively. The accumulative dissipated energy  $W_f$  when the specimen fractures, accumulative dissipated energy  $W_f^1$  at the initial stage of fatigue loading, accumulative dissipated energy  $W_f^2$  at the second stage and accumulative dissipated energy  $W_f^3$  at the acceleration stage increase with the increase in confining pressure, but stable energy dissipation per cycle  $w_d$  decreases. This may be due to the fact that as the confining pressure increases, the plasticity and ductility of the salt rock increases, and the fragility decreases (Song et al. 2013).

### 4.3 The Evolution Rule of the Rate of Dissipated Energy Change DER

The rate of dissipated energy change DER on the basis of the fatigued rock salt is calculated as shown in Fig. 8. DER versus load cycles shows an upward trend in the first stage

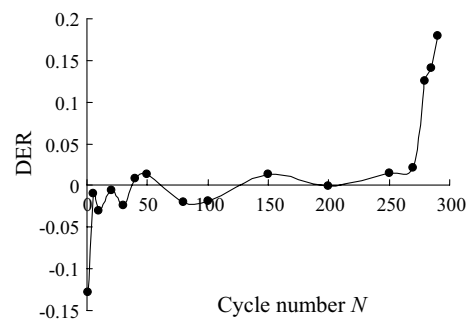


**Fig. 8** The DER evolution of rock salt for No.S1 specimen under fatigue loading at the stress level of 0.95

and is negative, whereas at the stable stage, DER only fluctuates around zero, and a stable value cannot be recognized. The result is inconsistent with that of asphalt mixtures, such as asphalt concrete and asphalt paint (Ghuzlan and Carpenter 2006; Lee et al. 2000; Tefpers et al. 1984). For asphalt mixtures, the value of DER at the stable stage is invariable and independent of the mixture type and the loading conditions; therefore, it is considered an important material parameter for describing damage. However, for rock salt, the energy dissipation at the stable stage is relatively stable under different applied stress amplitude, loading frequency and loading rate, and DER is about zero; thus, this method is not applicable for rock salt, as well as cement concrete (Lei et al. 2017), and is mainly applicable for asphalt mixtures. Essentially, the difference between rock salt and asphalt mixtures, such as asphalt concrete, asphalt paint, etc., results from different physical properties. The asphalt mixture is a mixture of asphalt and aggregate, whereas the rock salt consists of very high purity of NaCl and  $\text{Na}_2\text{SO}_4$  and a spot of  $\text{K}_2\text{SO}_3$ ; the different composition results in the viscoelasticity of the asphalt mixture and the ductility of rock salt, thus making the dissipation mechanism of the hysteretic energy also different. For the asphalt mixture, the hysteretic energy is mainly dissipated through heat release. However, for the salt rock, the hysteretic energy is mainly dissipated due to crack growth and the accumulative damage with consecutive cycles.

## 5 Fatigue Life Prediction Based on the Energy Method

The lifetime of fatigued rock salt can be predicted by the evolution law of the dissipated energy. The energy dissipation per cycle under different fatigue loading conditions remains constant throughout the second stage, and cycle number of the second stage occupies the major part of the total cycle number. It is found that the energy dissipation per cycle  $w_d$  at the stable stage increases linearly as the value

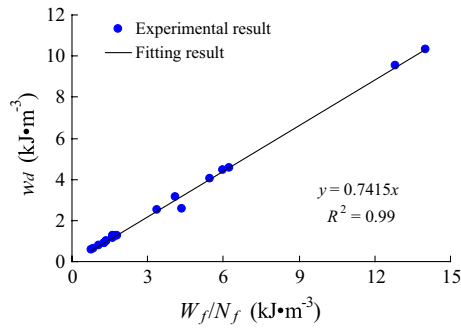


**Fig. 9** The linear fitting between  $W_f/N_f$  and  $w_d$  with a coefficient of correlation  $R^2$  of 0.99

of  $W_f/N_f$  increases as shown in Fig. 9. In addition, the relation is invariable and independent of the loading condition (the applied stress amplitude, loading frequency and loading rate). Therefore, the slope of the curve of  $w_d - W_f/N_f$  can be regarded as a constant, and its value can be expressed as

$$\xi = \frac{w_d N_f}{W_f} \tag{7}$$

where  $\xi$  is a constant,  $\xi = 0.7416$ . In addition, for the rock salt, the value of  $\xi$  is independent of loading conditions; from that, the fatigue life function based on Eq. (7) can be obtained as

$$N_f = \xi \frac{W_f}{w_d} \tag{8}$$

The relation between the fatigue life  $N_f$  and the loading conditions (the applied stress amplitude, loading frequency and loading rate) can be extracted by combining Eqs. (5) and (8):

$$N_f = \xi \frac{W_f}{c(\mu\nu)^a \exp [b(A - \sigma_3)]} \tag{9}$$

Substituting Eq. (9) into Eq. (6), the accumulative dissipated energy  $W_d^N$  at the current cyclic number  $N$  can be obtained as

$$W_d^N = \frac{Nc(\mu\nu)^a \exp [b(A - \sigma_3)]}{\xi} \tag{10}$$

Calculating the average of all the failure dissipated energy  $W_f$  in Fig. 8, we obtain that  $W_f = 233 \text{ kJ m}^{-3}$ . Substituting that into Eq. (9) and Eq. (10), the corresponding  $N_f - \mu\nu$ ,  $N_f - (A - \sigma_3)$  and  $W_d^N - N$  curves are obtained and shown in Figs. 10 and 11, respectively. It can be observed that these curves obtained from the proposed energy method are consistent with the test results.

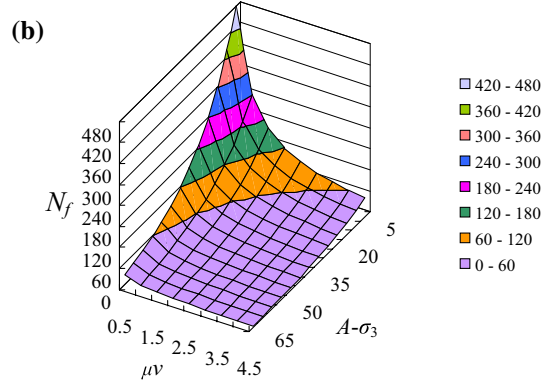
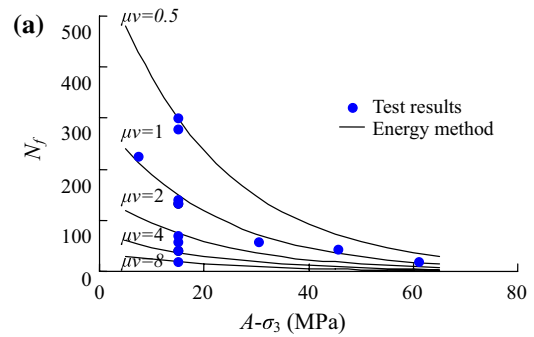


**Fig. 10**  $N_f$  curve based on the evolution rule of energy dissipation

### 6 Conclusion

1. The evolution of energy dissipation per cycle under fatigue loading is divided into three stages: the initial stage, the second stage and the acceleration stage. In the second stage, the energy dissipation per cycle remains stable and shows an exponential relation with the stress amplitude.
2. As an intrinsic characteristic of rock salt, the failure accumulative dissipated energy can be regarded as a failure criterion of fatigued rock salt and is independent

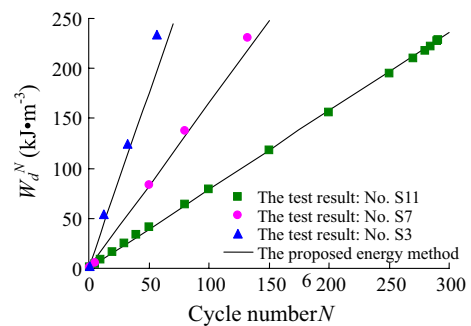


**Fig. 11**  $W_d^N - N$  curve based on the evolution rule of energy dissipation



of the applied stress amplitude, loading frequency and loading rate.

3. The model for prediction of fatigue life versus stress amplitude, frequency, confining pressure and loading rate is proposed for rock salt based on the stability of the energy dissipation per cycle and invariance of the failure energy dissipation. Comparison between the prediction and experimental results illustrates that the fatigue life can be estimated and predicted from this model.
4. The equation is proposed to calculate the accumulative dissipated energy of rock salt based on invariance of the failure energy dissipation and the stability of the energy dissipation per cycle. The proposed equation is validated by the comparison between its prediction results and the experimental results.

**Acknowledgements** This study is sponsored by the National Natural Science Foundation of China (Nos. 51179153 and 11572246). The financial support provided by these sponsors is greatly appreciated.

## References

- Dattoma V, Giancane S (2013) Evaluation of energy of fatigue damage into GFRC through digital image correlation and thermography. *Compos Part B Eng* 47:283–289
- Erarslan N (2016) Microstructural investigation of subcritical crack propagation and Fracture Process Zone (FPZ) by the reduction of rock fracture toughness under cyclic loading. *Eng Geol* 208(24):181–190
- Ghuzlan KA, Carpenter SH (2006) Fatigue damage analysis in asphalt concrete mixtures using the dissipated energy approach. *Can J Civ Eng* 33(7):890–901
- Guo YT, Yang CH, Mao HJ (2012) Mechanical properties of Jintan mine rock salt under complex stress paths. *Int J Rock Mech Min Sci* 56:54–61
- Hakan A (2009) Percolation model for dilatancy-induced permeability of the excavation damaged zone in rock salt. *Int J Rock Mech Min Sci* 46:716–724
- Kittitep F, Decho P (2010) Effects of cyclic loading on mechanical properties of Maha Sarakham salt. *Eng Geol* 112:43–52
- Lee HJ, Daniel JS, Kim YR (2000) Continuum damage mechanics-based fatigue model of asphalt concrete. *J Mater Civ Eng* 12(2):105–112
- Lei D, Zhao JH, Gong M, Yu DK (2008) On the energy dissipation in fatigue process and fatigue life prediction. *J Exp Mech* 5:008
- Lei D, Zhang P, He JT, Bai PX, Zhu FP (2017) Fatigue life prediction method of concrete based on energy dissipation. *Constr Build Mater* 145:419–425
- Liang WG, Zhao YS, Xu SG, Dusseault MB (2011) Effect of strain rate on the mechanical properties of salt rock. *Int J Rock Mech Min Sci* 48:161–167
- Liang WG, Zhang CD, Gao HB, Yang XQ, Xu SG, Zhao YS (2012) Experiments on mechanical properties of salt rocks under cyclic loading. *J Rock Mech Geotech Eng* 4(1):54–61
- Ma LJ, Wang MY, Zhang N, Fan PX, Li J (2017) A variable-parameter creep damage model incorporating the effects of loading frequency for rock salt and its application in a bedded storage cavern. *Rock Mech Rock Eng* (First Online: 05 June 2017)
- Payten WM, Dean DW, Snowden KU (2010) A strain energy density method for the prediction of creep-fatigue damage in high temperature components. *Mater Sci Eng A* 527:1920–1925
- Qian HT, Tan ZS, Li SD, Wang SJ (2010) Analysis of effect of stress on dissolution mechanism of salt rock. *Chin J Rock Mech Eng* 29(4):757–764
- Roberts LA, Buchholz SA, Mellegard KD, Düsterloh U (2015) Cyclic loading effects on the creep and dilation of salt rock. *Rock Mech Rock Eng* 48(6):2581–2590
- Shen SH, Airey GD, Carpenter SH, Hai H (2006) A dissipated energy approach to fatigue evaluation. *Road Mater Pavement Des* 7(1):47–69
- Song R, Yueming B, JingPeng Z, Deyi J, Chunhe Y (2013) Experimental investigation of the fatigue properties of salt rock. *Int J Rock Mech Min Sci* 64:68–72
- Tepfers R, Hedberg B, Szczekocki G (1984) Absorption of energy in fatigue loading of plain concrete. *Matériaux et Construction* 17(1):59–64
- Wang RZ, Zhang XC, Tu ST, Zhu SP, Zhang CC (2016) A modified strain energy density exhaustion model for creep-fatigue life prediction. *Int J Fatigue* 90:12–22
- Xiao L, Gu HC (1998) Plastic energy dissipation model for lifetime prediction of Zirconium and Zircaloy-4 fatigued at RT and 400 C. *J Eng Mater T ASME* 120(4):114–118
- Xiao JQ, Ding DX, Gen X (2009) Inverted S-shaped model for nonlinear fatigue damage of rock. *Int J Rock Mech Min Sci* 46:643–648
- Xiao JQ, Ding DX, Jiang FL, Gen X (2010) Fatigue damage variable and evolution of rock subjected to cyclic loading. *Int J Rock Mech Min Sci* 47:461–468
- Xie HP, Peng RD, Ju Y (2004) Energy dissipation of rock deformation and fracture. *Chin J Rock Mech Eng* 23(21):3565–3570
- Xie HP, Peng RD, Ju Y, Zhou HW (2005) On energy analysis of rock failure. *Chin J Rock Mech Eng* 24(15):2603–2608
- Xie HP, Li LY, Ju Y, Peng RD, Yang YM (2011) Energy analysis for damage and catastrophic failure of rock. *Sci China Technol Sci* 54(S1):199–209